Available online at www.sciencedirect.com
ScienceDirect
Journal of Power Sources 181 (2008) 281–286
JOURNAL OF POWER SOURCES
www.elsevier.com/locate/jpowsour

Short communication

Lanthanum oxide-coated stainless steel for bipolar plates in solid oxide fuel cells (SOFCs)

Jong Seol Yoon [a], Jun Lee [a], Hae Jin Hwang [a,*], Chin Myung Whang [a], Ji-Woong Moon [b], Do-Hyeong Kim [c]

[a] *School of Materials Science and Engineering, Inha University, 253 Yonghyun-dong, Nam-gu, Incheon 402-751, Republic of Korea*
[b] *Korea Institute of Ceramic Engineering and Technology, Seoul 153-801, Republic of Korea*
[c] *Research Institute of Industrial Science and Technology (RIST), Pohang, Republic of Korea*

Received 22 October 2007; received in revised form 10 December 2007; accepted 11 December 2007
Available online 12 February 2008

Abstract

Solid oxide fuel cells typically operate at temperatures of about 1000 °C. At these temperatures only ceramic interconnects such as $LaCrO_3$ can be employed. The development of intermediate-temperature solid oxide fuel cells (IT-SOFCs) can potentially bring about reduced manufacturing costs as it makes possible the use of an inexpensive ferritic stainless steel (STS) interconnector. However, the STS suffers from Cr_2O_3 scale formation and a peeling-off phenomenon at the IT-SOFC operating temperature in an oxidizing atmosphere. Application of an oxidation protective coating is an effective means of providing oxidation resistance. In this study, we coated an oxidation protective layer on ferritic stainless steel using a precursor solution prepared from lanthanum nitrate, ethylene glycol, and nitric acid. Heating the precursor solution at 80 °C yielded a spinable solution for coating. A gel film was coated on a STS substrate by a dip coating technique. At the early stage of the heat-treatment, lanthanum-containing oxides such as La_2O_3 and La_2CrO_6 formed, and as the heat-treatment temperature was increased, an oxidation protective perovskite-type $LaCrO_3$ layer was produced by the reaction between the lanthanum-containing oxide and the Cr_2O_3 scale on the SUS substrate. As the concentration of La-containing precursor solution was increased, the amount of La_2O_3 and La_2CrO_6 phases was gradually increased. The coating layer, which was prepared from a precursor solution of 0.8 M, was composed of $LaCrO_3$ and small amounts of $(Mn,Cr)O_4$ spinel. A relatively dense coating layer without pin-holes was obtained by heating the gel coating layer at 1073 K for 2 h. Microstructures and oxidation behavior of the La_2O_3-coated STS444 were investigated.
© 2008 Elsevier B.V. All rights reserved.

Keywords: Solid oxide fuel cell; $LaCrO_3$; Interconnector; STS444; Oxidation protective coating

1. Introduction

A fuel cell is an electrochemical energy conversion device that can directly convert supplied chemical energy (i.e., fuel) to electrical energy (i.e., electricity). Fuel cells have many advantages, including high energy conversion efficiency, high power density, and relatively low pollution emissions [1,2]. Among the various types of fuel cells, solid oxide fuel cells (SOFCs) have a number of other specific advantages. SOFCs require no fuel reformer, because their operating temperature is around 1273 K. In addition, the efficiency of SOFCs can be increased by co-generation systems [2]. However, the high operating temperature can also cause several serious problems. It leads to long-term cell performance degradation (thus affecting long-term reliability). This is associated with inter-diffusion between SOFC-constituting components and thermal shock by high temperature cycles. Recently, many groups have been studying intermediate-temperature (IT) SOFCs having good performances at lower temperature [3,4]. Some cheaper metal alloys can replace established ceramic-based interconnector, if the operating temperature of the SOFCs can be lowered to around 873–1073 K [5,6].

Several properties are required for interconnector materials: (1) high electrical conductivity with no ionic conduction; (2) thermal expansion compatibility with other components such as the electrolyte, electrodes, and sealing glass; (3) good corrosion

* Corresponding author. Tel.: +82 32 860 7521; fax: +82 32 862 4482.
E-mail address: hjhwang@inha.ac.kr (H.J. Hwang).

0378-7753/$ – see front matter © 2008 Elsevier B.V. All rights reserved.
doi:10.1016/j.jpowsour.2007.12.053

resistance in oxidizing and reducing atmospheres; (4) suitable stability of chemical reaction with other components; and (5) dense and good mechanical strength. Given these requirements, metallic interconnectors offer considerable benefit. However, oxide scales are continuously produced at high operation temperature and, because of a thermal expansion mismatch between the scale and interconnector, the scales easily peel-off from the interconnector. This is a very important issue with regard to application of metallic interconnectors to SOFCs.

In general, oxide scales, such as Al_2O_3, SiO_2, and Cr_2O_3, are formed on metallic alloys. The electrical conductivity of SiO_2 and Al_2O_3 are lower than Cr_2O_3. Therefore, Cr_2O_3-former alloys, which are composed of 17–26 wt% Cr, have been proposed as a metallic interconnector material. However, there are two important issues that must be addressed prior to use of Cr_2O_3-former alloys for metallic interconnector. The first is Cr_2O_3 oxide, which is generated on the Cr_2O_3-former alloys and has a high electrical resistance of about $1 \times 10^2\ \Omega$ cm at 1073 K [7]. The second is the Cr_2O_3 scale derived from the Cr-former alloys produces volatile Cr species. They are often reduced and segregated at triple-phase boundaries and inhibit the cathode reaction kinetics [8,9].

In order to prevent the formation of Cr_2O_3 scale, application of a reactive element oxide coating on the metallic interconnector has been attempted. The reactive element oxide can change the oxide scale formation mechanism on the Cr_2O_3-forming alloy. Reactive elements such as La, Nd, Sm, Gd, Yb, and Y can produce an electrically conductive perovskite phase on the Cr_2O_3-former alloy in an oxidizing atmosphere [10,11]. Generally, the addition of a small amount of a rare-earth element improves the oxidation resistance of the Cr_2O_3-forming alloy. In this paper, a reactive oxide layer, lanthanum oxide, was coated on a commercial ferritic-stainless steel plate (STS444) by an ethylene glycol process. Heating the lanthanum-containing gel coating layer results in the formation of a perovskite-type $LaCrO_3$ on the STS444. Microstructure and oxidation behavior of the $LaCrO_3$-coated STS444 were investigated in terms of concentration of the precursor solution and heat-treatment conditions.

2. Experimental procedure

A precursor solution for the protective coating layer was prepared by an ethylene glycol process [12]. Ethylene glycol (Kanto Chemical Co., 99%) was used as a solvent and also as a chelating agent after reacting with nitric acid. The starting material was lanthanum(III) nitrate hexahydrate ($La(NO_3)\cdot 6H_2O$, GFS Chemicals Inc., 99%). An appropriate amount of $La(NO_3)\cdot 6H_2O$ was dissolved in 40 cm^3 of ethylene glycol and 5 cm^3 of nitric acid was subsequently introduced to the solution. The solution was heated and stirred on a hot plate, which was controlled at a uniform temperature of 353 K for 1 day. A spinable precursor solution having various La concentrations was obtained.

A commercial ferritic-stainless steel STS444, which has a chemical composition of 18.59 Cr, 1.96 Mo, 0.26 Si, and 0.24 Mn was used as a substrate. The STS444 plate was cut into pieces having dimensions of 10 mm × 50 mm × 1.5 mm via a wire cutting machine. The STS444 surfaces were then polished with a series of increasingly finer grit SiC papers (from #400 to 2000), and finally with a diamond paste (from 3 to 1 μm) in order to obtain a mirror surface. The polished substrates were ultrasonically cleaned in acetone and ethanol for 10 min, respectively. They were subsequently rinsed in distilled water, soaked for 30 s in acetone, and dried with a nitrogen gas gun. Finally, the substrates were dried on a hot plate at 373 K.

A dip coating technique was applied to form a gel coating layer on the substrate. The substrate was immersed into a precursor solution for 1 min and was removed from the solution at a constant linear speed of 0.066 mm s^{-1}. The coated substrate was then dried successively at 353 and 673 K on a hot plate. These procedures were repeated three times to increase the film thickness. To form a desired oxide coating layer ($LaCrO_3$ perovskite phase), the coated substrate was heat-treated at 1073 K for 2 h.

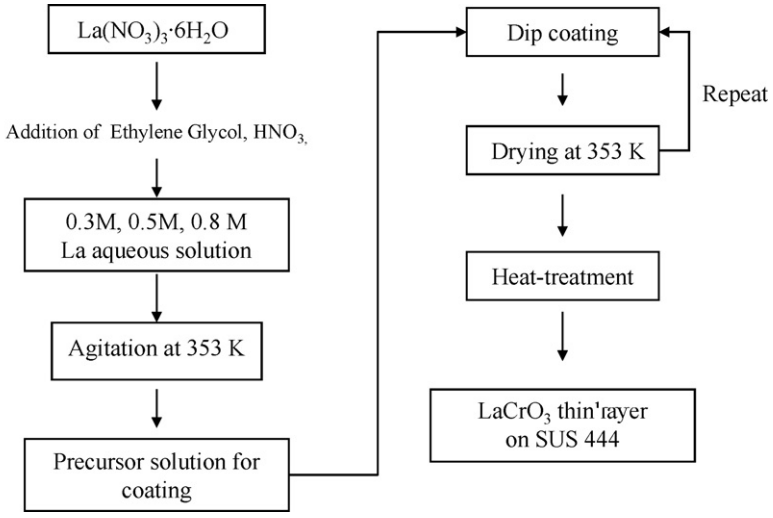

Fig. 1. Procedure for fabrication of $LaCrO_3$ coating layer.

The heating speed was 2 °C min^{-1}. The experimental procedure described above is outlined in Fig. 1.

Phase identification of heat-treated and subsequently oxidized STS444 surfaces was carried out with a thin film X-ray diffractometer (Philips, X'pert MPD) using Ni-filtered Cu Kα radiation. Surface and cross-sectional images of the coated layer were observed by scanning electron microscopy (SEM, HITACH, S-4300).

3. Results and discussion

Phase evolution as a function of heat-treatment temperature in La-coated STS444 is shown in Fig. 2. The coating layer was prepared from a precursor solution of 0.3 M. After heat-treatment at 773 K, the surface of the sample consisted of La_2CrO_6, La_2O_3 and a $LaCrO_3$ perovskite phase appeared. This means that the perovskite phase formed at a temperature between 673 and 773 K. As the heat-treatment temperature was increased, the La_2O_3 disappeared and the relative intensity of the La_2CrO_6 was decreased. On the other hand, the $LaCrO_3$ perovskite showed a stronger intensity. The formation mechanism of the $LaCrO_3$ perovskite is as follows: a dried gel coating layer on STS444 is crystallized into La_2O_3 above 673 K and the La_2O_3 reacts with Cr_2O_3, which is formed between the coating layer and STS444 substrate during heat-treatment, producing a La_2CrO_6 phase at temperature lower than 673 K. It appears that the $LaCrO_3$ perovskite phase results from the reaction between the La_2CrO_6 and Cr_2O_3 above 773 K. With increasing heat-treatment temperature, considerably more $LaCrO_3$ phase is formed on STS444, because the formation of the Cr_2O_3 phase would be further accelerated at high temperatures.

The sample that was heat-treated at 973 K mainly consists of $LaCrO_3$ and chrome-manganese spinel while very small amounts of Cr_2O_3 were also detected. The Mn/Cr atomic ratio of the chrome-manganese spinel was determined to be approximately 1/1–1/2 by EDAX analysis. Hence, we refer to the chrome-manganese spinel as $(Mn,Cr)_3O_4$ in this paper. The formation of the $(Mn,Cr)_3O_4$ spinel is thought to be caused by the presence of outward-diffused Cr and Mn species from STS444. Some Cr_2O_3 is consumed for $LaCrO_3$ formation during the heat-treatment. At the same time, the Mn would be dissolved in the Cr_2O_3 to produce the $(Mn,Cr)_3O_4$ spinel phase.

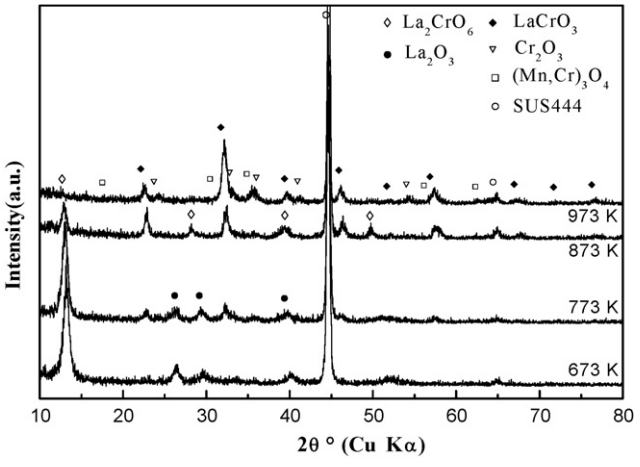

Fig. 2. X-ray diffraction patterns of coated STS444 heat-treated at various temperatures for 2 h (the concentration of the precursor solution is 0.3 M).

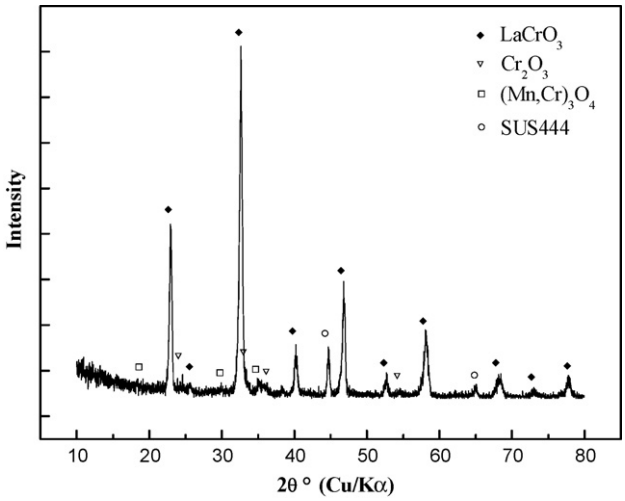

Fig. 3. X-ray diffraction pattern of coated SUS444 heat-treated at 1073 K for 2 h (the concentration of the precursor solution is 0.8 M).

In order to form a secondary phase-free perovskite coating layer and also to improve the coating layer's density, we prepared three kinds of precursor solutions having different lanthanum concentration (0.3, 0.5, and 0.8 M La). Fig. 3 shows the XRD pattern of a coated STS444 that was prepared from a precursor solution of 0.8 M La. In contrast with the samples prepared from 0.3 and 0.5 M La solutions, the 0.8 La sample was prepared by a single coating/drying process. The XRD pattern indicates a well defined $LaCrO_3$ perovskite phase, although small amounts of the spinel phase remain. Better crystallization of the $LaCrO_3$ phase observed in the 0.8 M La-coated STS444 might be due to a dense microstructure and grain growth at high temperature (this sample was heat-treated at 1073 K). In addition, the grain size of the coating layer from the 0.8 M La precursor solution is much larger than those of the coating layer from 0.3 and 0.5 M La precursor solutions, as described in greater detail below.

Fig. 4 shows the surface microstructure of the coating layers on STS444 after heat-treatment at 973 K for 2 h. The $LaCrO_3$ coating layer from the 0.3 M La precursor solution is somewhat rough and irregular sized grains can be observed in the microstructure. On the other hand, the $LaCrO_3$ from the 0.8 M La precursor solution has a denser and more homogeneous microstructure than the 0.3 and 0.5 M La solutions. The grain size of $LaCrO_3$ is increased with an increase of the concentration of the precursor solution. The porosity, i.e., the density of the coating layer, can be a very important factor in terms of influencing the oxidation resistance of STS444, particularly if the pores are opened. The effect of microstructure on the oxidation behavior of the coating layer is described later.

Cross-sectional SEM images of the coating layers from 0.5 M (a) and 0.8 M (b) La solution samples heat-treated at 973 K for 2 h are shown in Fig. 5. The LSC coating layers are well adhered to the substrate. As noted before, we repeated the coating/drying process three times in the case of the 0.3 and 0.5 M La precursor

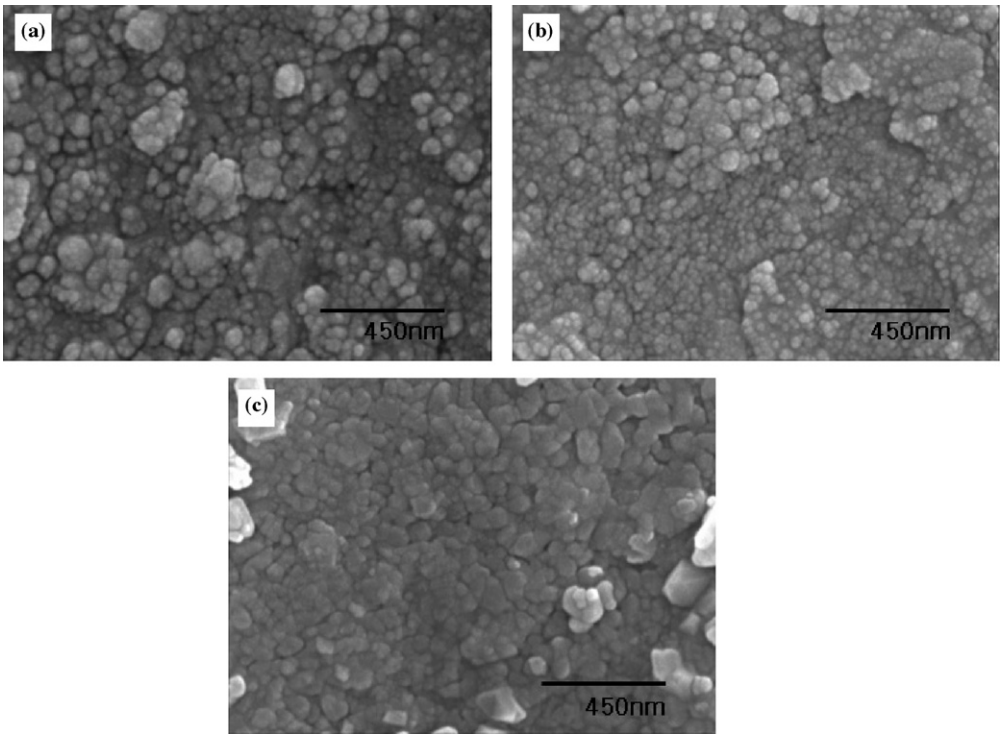

Fig. 4. Scanning electron micrographs of $LaCrO_3$ coating layer on STS444 substrate prepared from a precursor solution of 0.3 M (a), 0.5 M (b), and 0.8 M (c) (the samples were heat-treated at 973 K for 2 h).

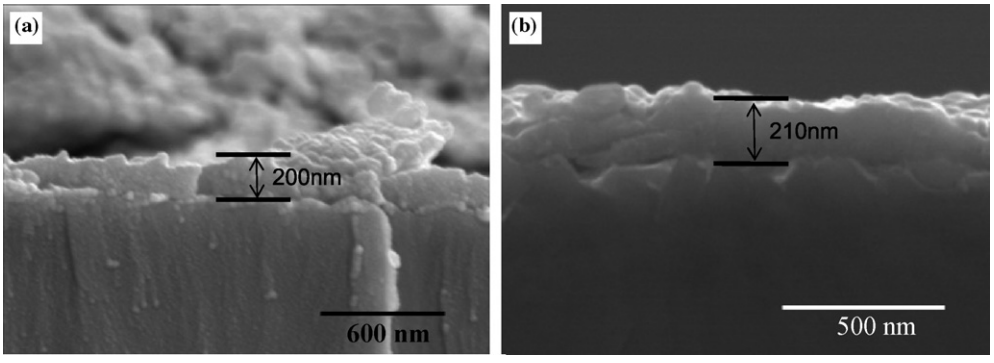

Fig. 5. Cross-sectional scanning electron micrographs of $LaCrO_3$ coating layer on STS444 substrate prepared from a precursor solution of 0.5 M (a) and 0.8 M (b) (the samples were heat-treated at 973 K for 2 h).

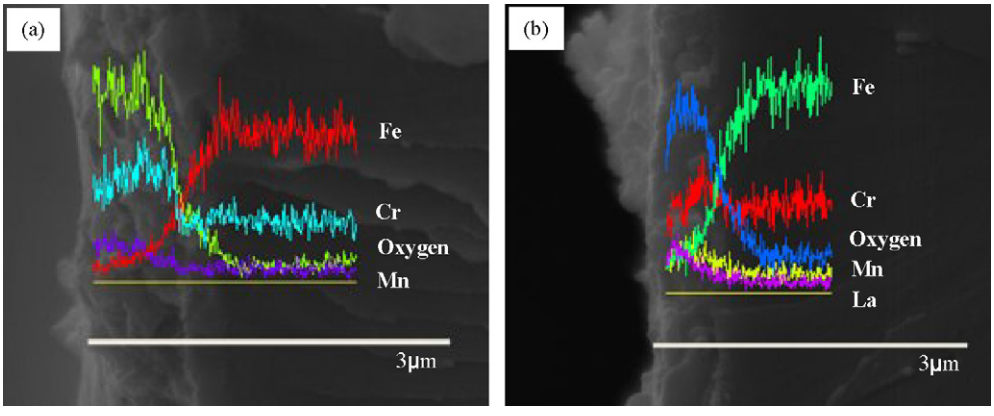

Fig. 6. EDAX analysis of uncoated (a) and $LaCrO_3$-coated SUS444 (b) oxidized at 973 K for 500 h (the coating layer was prepared from a precursor solution of 0.8 M).

solutions, while the gel coating from the 0.8 M La solution was obtained by only a single coating/drying step. The thickness of the coating layer is estimated to be approximately 200 nm for all samples. This suggests that the thickness of the coating layer obtained by single coating/drying is much larger in the 0.8 M La solution than after one iteration of the coating process for the 0.3 and 0.5 M La solutions. The thickness of the coating layer is closely related with viscosity of the precursor solution and also the coating/drying time. According to the numerical formula relating thickness with viscosity ($t = K(\eta\upsilon/\rho g)^{1/2}$, where t = film thickness, K = a constant, η = viscosity of the solutions, υ = rate of pulling up, and ρ = density of the solution) [13], the thickness of the film is proportional to the viscosity of the solution. In this study, the viscosity of the precursor solutions was measured to be 34, 39, and 84 cP for the 0.3, 0.5, and 0.8 M solutions, respectively. It is evident that larger thickness of the 0.8 M La solution results from its high viscosity.

Fig. 6 shows cross-sectional SEM images and EDAX line analysis profiles of the uncoated and 0.8 M La-coated STS444 oxidized at 973 K for 500 h. Comparing Fig. 6(b) and (a), it can be inferred that the outward diffusion of Cr and Mn is effectively depressed by the presence of the $LaCrO_3$ coating layer. As is evident from Fig. 6(b), a Mn- and La-rich top layer is found while a Cr-rich layer is located between the top layer and the SUS444 substrate. This suggests that the Cr_2O_3 is formed between the $LaCrO_3$ or $(Mn,Cr)_3O_4$ spinel and STS444 substrate. However, it is still unclear at the moment as to where the $(Mn,Cr)_3O_4$ phase is because of the uncertainty of spatial resolution for EDAX analysis. According to findings reported in the literature, the formation of the $(Mn,Cr)_3O_4$ indicates the outward diffusion of Mn from the stainless steel substrate. The Mn–Cr spinel is formed at the top surface of the STS444 substrate, because the diffusivity of Mn is much faster than Cr [14–18]. EDAX and XRD analysis results are in accordance with reported results. Therefore, it can be speculated that the $(Mn,Cr)_3O_4$ phase is located between $LaCrO_3$ and Cr_2O_3 and some spinel phases also exist in the surface of the oxidized samples (please see prismatic grains in Fig. 8(a) and (c)).

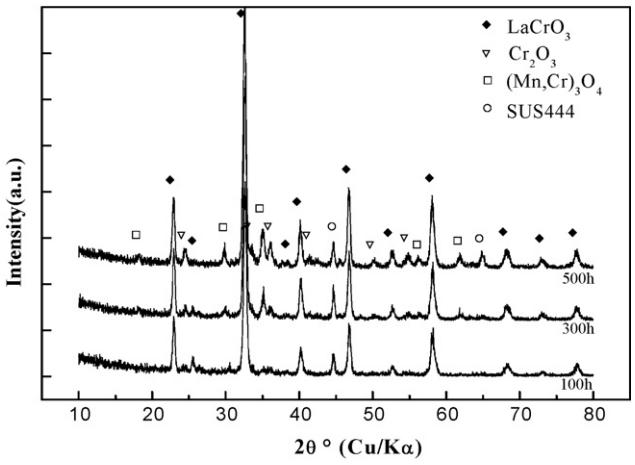

Fig. 7. X-ray diffraction patterns of $LaCrO_3$-coated STS444 oxidized at 973 K for 100, 300, and 500 h (the coating layer was prepared from a precursor solution of 0.8 M).

Oxidation behavior is also confirmed by XRD patterns of the $LaCrO_3$-coated STS444 oxidized at 973 K for 100, 300, and 500 h, respectively. Thin film XRD patterns shown in Fig. 7 indicate a gradual growth of Cr_2O_3 and $(Mn,Cr)_3O_4$ spinel with respect to the oxidation time. Comparing the 500 h-oxidized

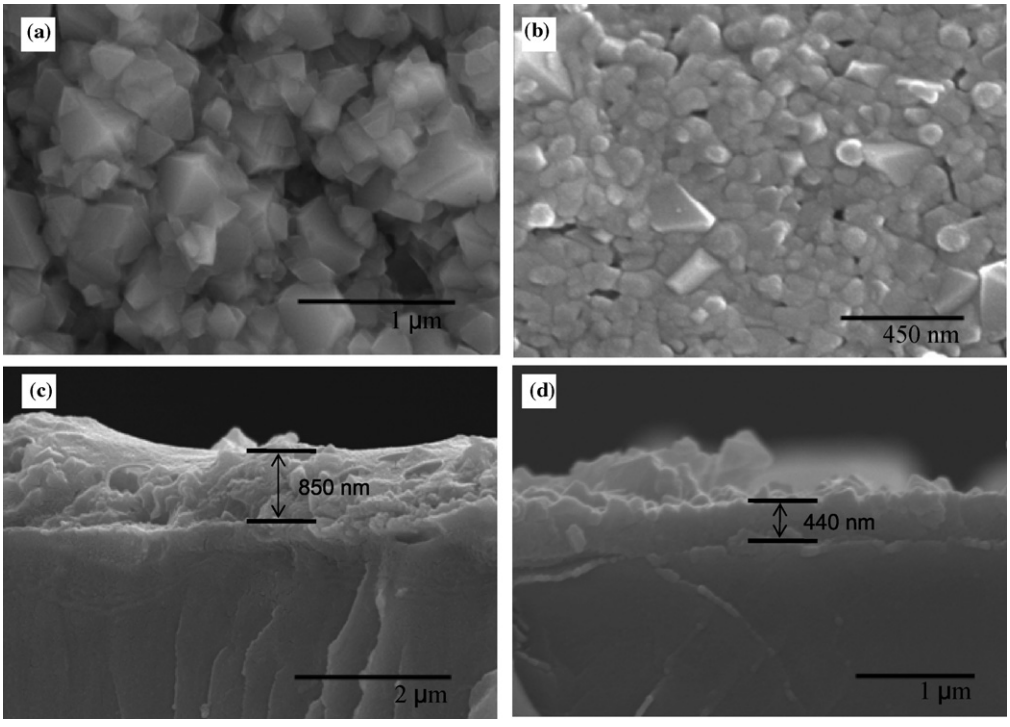

Fig. 8. Surface and cross-sectional morphology of uncoated and $LaCrO_3$-coated STS444 oxidized at 973 K for 500 h (the coating layer was prepared from a precursor solution of 0.8 M); (a) and (c) uncoated samples, (b) and (d) coated samples.

sample with 300 h sample, the relative intensity of the Cr_2O_3 increases more than that of the $(Mn,Cr)_3O_4$ spinel. This result is considered to be due to the pore formation in $LaCrO_3$ coating layer of 500 h-oxidized sample, which will be described next paragraph. In addition, grain growth of $(Mn,Cr)_3O_4$ spinel may occur, whereby the relative intensity of the spinel peaks increases with oxidation time.

Surface morphology and cross-sectional SEM images of uncoated and $LaCrO_3$-coated STS444 after oxidization at 973 K for 500 h are shown in Fig. 8. The surface layer of the uncoated STS444 is found to be $(Mn,Cr)_3O_4$ spinel and it shows a porous microstructure with large spinel grains. In the case of $LaCrO_3$-coated STS444, $LaCrO_3$ grains and inter-granular pores become much larger after oxidation (compare Fig. 8 with Fig. 4). Grain growth without densification leads to pore growth. Although the porosity of the coating layer is not high, pores may provide an oxygen transport path, which accelerates the inward diffusion of oxygen and the continuous growth of Cr_2O_3 during oxidation. As described before, the formation of a Cr_2O_3 layer between $LaCrO_3$ and the STS444 substrate might be associated with pore growth as oxidation proceeds.

The thickness of the oxide scale of uncoated STS444 after oxidization for 500 h is estimated to be 850 nm. Note also that the growth of the surface layer of $LaCrO_3$-coated STS444 was significantly inhibited by the $LaCrO_3$ coating layer, although it did increase from 200 to 400 nm. These results indicate that the oxidation resistance of the $LaCrO_3$-coated STS444 specimen is superior to that of the uncoated sample. It is believed that Cr_2O_3 layer growth, which may be due to the inward diffusion of oxygen, and also the growth of the $LaCrO_3$ layer by further reaction between La_2O_3 and Cr_2O_3 (if unreacted La_2O_3 is present in the coating layer) as well as coarsening of the $LaCrO_3$ grains, may be responsible for the surface layer growth.

4. Conclusions

A La-based gel film was successfully coated on a STS444 substrate by a dip coating technique and $LaCrO_3$ perovskite phase was formed by heat-treating the gel film at 773–1073 K. Transient phases such as La_2O_3 and La_2CrO_6, which were formed at lower temperature, reacted with Cr_2O_3 to produce $LaCrO_3$ perovskite. It is believed that control over the reaction between La_2O_3 or La_2CrO_6 and Cr_2O_3 by modification of the precursor solution and heat-treatment temperature is an effective means of producing a dense and thick $LaCrO_3$ coating layer on the STS substrate. Higher viscosity resulted in a thicker gel coating layer. In order to increase the film thickness, the precursor solution should be further modified. During oxidation $(Mn,Cr)O_4$ spinel and Cr_2O_3 phases were formed on STS444. The spinel and Cr_2O_3 might result from outward diffusion of Mn and inward diffusion of oxygen, respectively. As a consequence, large spinel grains were produced at the top surface of the STS444 while growth of a Cr_2O_3 layer occurred between the $LaCrO_3$ coating layer and STS444. Compared with non-coated SUS444, the oxidation resistance of $LaCrO_3$-coated STS444 was significantly improved.

Acknowledgement

This work was supported by an INHA UNIVERSITY Research Grant.

References

[1] N.Q. Minh, T. Takahash, Science and Technology of Ceramic Fuel Cell, 1st ed., Elsevier Science, Amsterdam, 1995, pp. 1–40.
[2] B.C.H. Steele, Nature 414 (15) (2001) 345–352.
[3] Y.H. Lim, J. Lee, J.S. Yoon, C.E. Kim, H.J. Hwang, J. Power Sources 171 (19) (2007) 79–85.
[4] D. Prakash, T. Delahaye, O. Joubert, M.-T. Caldes, Y. Piffard, J. Power Sources 167 (1) (2007) 111–117.
[5] T. Kadowaki, T. Shiomitsu, E. Matsuda, H. Nakagawa, H. Tsuneizumi, T. Maruyama, Solid State Ionics 67 (1993) 65–69.
[6] T. Brylewski, M. Nanko, T. Maruyama, K. Przybylski, Solid State Ionics 143 (2001) 131–150.
[7] G.V. Samsonov, The Oxide Handbook, 2nd ed., IFI/Plenum Data Company, New York, 1982, pp. 125.
[8] H. Tu, U. Stimming, J. Power Sources 127 (2004) 284–293.
[9] A. Webber, et al., J. Power Sources 127 (2004) 273–283.
[10] S. Chevalier, J.P. Larpin, Acta Mater. 50 (2002) 3105–3114.
[11] M. Stanislcwski, J. Froitzhein, et al., J. Power Sources 164 (2007) 578–589.
[12] C.C. Chen, M.M. Nasrallah, H.U. Anderson, J. Electrochem. Soc. 140 (12) (1993) 3555–3560.
[13] N.B. Dahotre, T.S. Sudarshan, Intermetallic and Ceramic Coating, Marcel Dekker, Inc., NY, 1999, pp. 40–51.
[14] X. Chen, P.Y. Hou, C.P. Jacobson, S.J. Visco, L.C.D. Jonghe, Solid State Ionics 176 (2005) 425–433.
[15] N. Sakai, et al., Solid State Ionics 176 (2005) 681–686.
[16] H. Kurokawa, K. Kawamura, T. Maruyama, Solid State Ionics 168 (2004) 13–21.
[17] K. Fujita, T. Hashimoto, K. Ogasawara, H. Kameda, Y. Matsuzaki, T. Sakurai, J. Power Sources 131 (2004) 270–277.
[18] J.W. Fergus, Mater. Sci. Eng. A 397 (2005) 271–283.